

INFLUENCE OF JOINT TYPE ON SHEAR BEHAVIOR OF SEGMENTAL CONCRETE BEAMS WITH EXTERNAL TENDONS

Dinh Hung NGUYEN^{*1}, Ken WATANABE^{*2}, Junichiro NIWA^{*3} and Tsuyoshi HASEGAWA^{*4}

ABSTRACT

This paper presents experimental results of segmental concrete beams with external tendons. The shear failure mechanism was investigated considering the effect of the prestress level and types of segmental joint. The experimental results showed that the shear failure mechanism of segmental concrete beams with dry joint was similar to that with epoxy joint at the ultimate stage. The experimental results from this study were compared with AASHTO and the modified model. The results from the modified model have a good agreement with experimental results.

Keywords: segmental concrete beam, external tendon, shear mechanism, dry joint, epoxy joint

1. INTRODUCTION

Precast segmental construction is widely used in bridge structures, because of substantial cost and time saving in construction. From the beginning, internal tendon technology has been used for segmental technology where tendons are located inside the concrete cross section. However, problems such as leakage at epoxy joints or corrosion in tendons may cause damage in segmental bridges. So, the application of external prestressing to precast segmental structures has been used as an innovative method in segmental concrete technology.

The sudden collapse of Koror-Babeldaob bridge [1] was an example of failure of a segmental concrete bridge. Shear problem is one of probable causes, explained in Reference [1], that have been accepted to describe the collapse of Koror-Babeldaob bridge. Shear carrying capacity of segmental beams has been predicted based on direct shear test [2, 3]. Zhou et al. [3] showed that shear carrying capacity of dry joints varied from 60% to 80% of that of epoxy joints in direct shear test. In addition, the effect of joint opening was not considered in direct shear test. Therefore, polymerization of epoxy [4] reduces shear carrying capacity of segmental beams with epoxy joint.

Segmental joint applied for segmental concrete beams is normally match-cast joint bonded with epoxy, called as epoxy joint. Match-cast segmental joint is also dry joint, in which no epoxy is applied, for segmental bridges wherever is possible to avoid the problems in epoxy joints [4]. The shear transfer across an opening joint is a very complex problem for precast segmental concrete beams with external tendons. As load passes to the limit stage, a segmental joint opens due to the lack of longitudinal reinforcements. The area at a segmental

joint to transfer shear force is reduced. It leads to the collapse of segmental beams. For these reasons, it is necessary to confirm that shear failure does not take place in the precast segmental concrete structure with epoxy joint or dry joint, especially at opening joints.

The objectives of this paper are to investigate the shear transfer mechanism of epoxy joint and dry joint. The shear failure mechanism of segmental concrete beams with external tendons, such as propagation of cracks, joint opening and shear carrying capacity is examined. Main parameters are prestressing force and joint types, i.e. epoxy joint or dry joint. The modified model [5], explained in Section 2, is verified in order to confirm its applicability for predicting the shear carrying capacity of segmental concrete beams with external tendons and dry joint.

2. LITERATURE REVIEW

Figure 1 shows two schematic diagrams of the modified model for predicting the shear carrying capacity of segmental concrete beams with external tendons and epoxy joint considering the joint position [5]. The parameter m , $m = \cot\theta$ and θ is the angle of the concentrated stress flow from the loading point inclining to the beam axis, is affected by the joint position. In Model 1, the distance md is defined as the horizontal distance from the loading point to the end node of strut member {3}. The strut member {4} is provided from the bottom of the web at the edge of the segmental joint to the loading point. In Model 2, the distance md is defined as the horizontal distance from the loading point to the end node of strut member {4}. The strut member {3} is provided from the bottom of the web at the edge of the segmental joint to the loading point. From the parametric study in FEM analysis [5],

*1 Ph.D. student, Dept. of Civil Engineering, Tokyo Institute of Technology, JCI Member

*2 Assistant Prof., Dept. of Civil Engineering, Tokyo Institute of Technology, Ph.D., JCI Member

*3 Prof., Dept. of Civil Engineering, Tokyo Institute of Technology, Dr. E., JCI Member

*4 Research Engineer, Research and Development Center, DPS Bridge Works Co., Ltd.

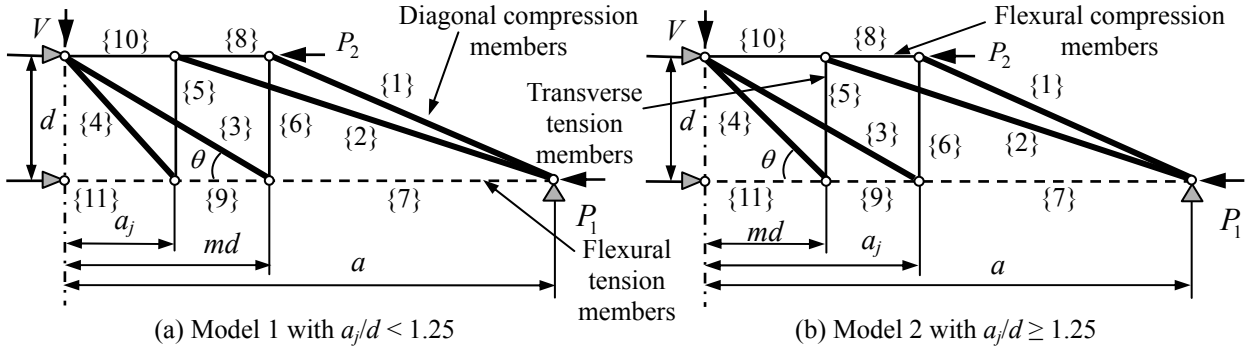


Fig. 1 Schematic diagrams of modified model.

the equation for estimating the value of m for Model 1 and Model 2 is expressed below in Eq. (1) and (2), respectively,

$$m = 1.395 \left(\frac{a_j}{d} \right)^{\frac{3}{10}} \left(\frac{a}{d} \right)^{\frac{3}{4}} (\sigma_l)^{-\frac{1}{4}} \quad (1)$$

$$m = 0.112 \left(\frac{a_j}{d} \right)^{\frac{5}{7}} \left(\frac{a}{d} \right)^{\frac{1}{4}} (\sigma_l)^{\frac{5}{9}} \quad (2)$$

where a_j is the distance from the critical segmental joint to the loading point; d is the effective depth of a beam; a is the shear span; σ_l is the lower extreme fiber stress.

The effects of loading plate, support plate and effective depth [6], stirrup [7], a/d and a_j/d ratios [5] were considered in formulating the horizontal thickness of a strut member. The horizontal thickness in the vicinity of loading point, t_l and support, t_s for Model 1 are shown in Eqs. (3) and (4), and the values of t_l and t_s for Model 2 are shown in Eqs. (5) and (6), respectively,

$$t_l = (w_l + 0.1d) \left(\frac{b_f}{b_w} \right)^{\frac{1}{5}} \left(1 + \left(\frac{A_{sv}}{b_w s} \right)^{\frac{1}{4}} \right) \left(0.167 \left(\frac{a}{d} \right)^{\frac{10}{7}} \left(1 + 0.025 \left(\frac{a_j}{d} \right)^{\frac{6}{5}} \right) \right) \quad (3)$$

$$t_s = 2(w_s + 0.1d) \left(\frac{b_f}{b_w} \right)^{\frac{1}{5}} \left(1 + \left(\frac{A_{sv}}{b_w s} \right)^{\frac{1}{4}} \right) \left(0.167 \left(\frac{a}{d} \right)^{\frac{10}{7}} \left(1 + 0.025 \left(\frac{a_j}{d} \right)^{\frac{6}{5}} \right) \right) \quad (4)$$

$$t_l = (w_l + 0.1d) \left(\frac{b_f}{b_w} \right)^{\frac{1}{5}} \left(1 + \left(\frac{A_{sv}}{b_w s} \right)^{\frac{1}{4}} \right) \left(0.174 \left(\frac{a}{d} \right)^{\frac{7}{5}} \left(1 + 0.004 \left(\frac{a_j}{d} \right)^{\frac{5}{5}} \right) \right) \quad (5)$$

$$t_s = 2(w_s + 0.1d) \left(\frac{b_f}{b_w} \right)^{\frac{1}{5}} \left(1 + \left(\frac{A_{sv}}{b_w s} \right)^{\frac{1}{4}} \right) \left(0.174 \left(\frac{a}{d} \right)^{\frac{7}{5}} \left(1 + 0.004 \left(\frac{a_j}{d} \right)^{\frac{5}{5}} \right) \right) \quad (6)$$

where, w_l is the loading plate width; w_s is the support plate width; b_f is the width of flange; b_w is the width of web; A_{sv} is the cross sectional area of stirrup; s is the spacing of stirrups.

In order to calculate the shear carrying capacity of segmental concrete beams with external tendons and epoxy joint, equivalent elastic analysis is utilized. The member force, F_i of each member is calculated based on Castigliano's second theorem, i.e. the theorem of minimum strain energy. The resistance of each member, R_i is calculated by multiplying f'_c by the softening parameter, η [6] and the correlatively cross sectional area, A_i . The shear carrying capacity is estimated when the maximum value of ratio of the F_i to R_i is equal to 1 [$\max (F_i/R_i) = 1, i = 1$ to 4].

The modified model [5] is proven to provide high accuracy and simplicity in predicting the shear carrying capacity of segmental concrete beams with external tendons and epoxy joint. However, it has not yet been extended to the segmental concrete beams with external tendons and dry joint. In addition, the modified model has limited applicability for segmental concrete beams with the concrete stress at the lower fiber greater or equal to 10 N/mm^2 .

3. TEST PROGRAM

3.1 Testing beams

Three simply supported concrete beams designed to fail in shear with a/d ratio of 3.5 were used. The beams consisted of two segments. The segmental joint was arranged in the tested shear span. The distance from the loading point to the joint position, a_j , used in these beams was $1.0d$, where d was the effective depth of the beam. Test specimens were T-shaped section concrete beams with the span length of 3.2 m. Two deviators 1.367 m apart were located symmetrically with respect to the midspan, as shown in Fig. 2(a). Different prestress levels and joint types were investigated in these beams. The concrete stress at the upper fiber of the all segmental beams was about 0 N/mm^2 . One segmental concrete beam with epoxy joint was prestressed to obtain the stress of 6 N/mm^2 at the lower fiber. The name of this beam with epoxy joint was SJ10-06. "SJ10" stands for the segmental joint with a_j of $1.0d$. Two other beams were segmental beams with dry joint. The two beams with dry joint were prestressed to obtain the concrete stress of 10 N/mm^2 and 6 N/mm^2 at the lower fiber. Therefore, the names of these beams were DSJ10-10 and DSJ10-06, respectively. "DSJ10" stands for the dry segmental joint

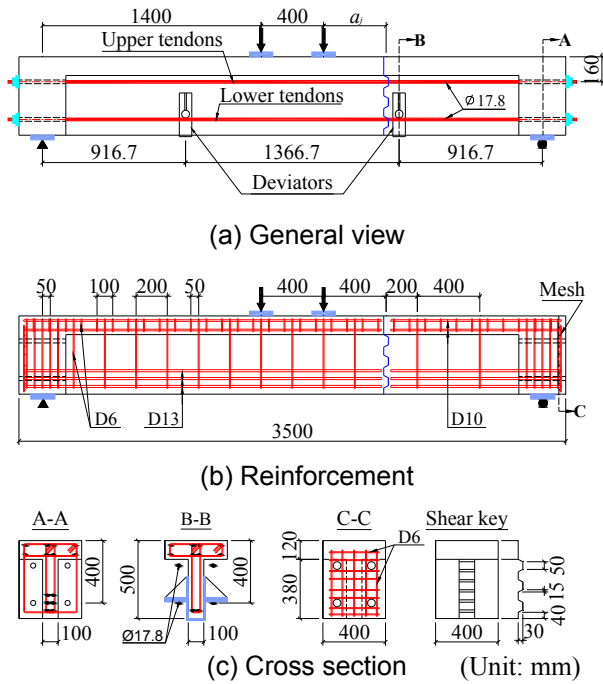


Fig. 2 Detail of specimens

with a_j of $1.0d$. The last two numbers in the name of the beams indicate the concrete stress at the lower fiber.

3.2 Materials

The arrangement of reinforcement in the beams is shown in Fig. 2(b). The non-prestressed steels were deformed bar of grade SD295A. Six deformed bars with a nominal diameter of 13 mm (D13) and eight deformed bars with a nominal diameter of 10 mm (D10) were provided as internal longitudinal bars at the bottom and top flange, respectively. The tested shear span, where the segmental joint was located, was reinforced by stirrups with a nominal diameter of 6 mm (D6) at an interval of 400 mm. The other shear span was reinforced with D6 stirrup at an interval of 200 mm. D6 stirrups were also used at the top flange with an interval of 100 mm. The mechanical properties of the steel bars are given in Table 1. Mesh reinforcement with D6 was utilized at the end of a beam to resist local stresses due to the prestressing force.

The match-cast method was used for casting the segmental beams. In this method, the large segment of each beam was cast first with a wood shear key as an end formwork. Two days later the formwork was removed and the large segment itself was used as an end formwork for the next casting in order to provide a perfect matching between the two segments. After casting, the concrete beams were cured at atmospheric condition. The design strength of concrete, f_c was specified as 65.0 N/mm^2 at 28 days. The actual compressive and tensile strengths of concrete are tabulated in Table 2.

The prestressing tendon used for the beams was of type SWPR19L $\phi 17.8$ mm. The yield and ultimate strengths of the tendon were 1760 N/mm^2 and 1950 N/mm^2 , respectively. The external tendons were placed

Table 1 Mechanical properties of reinforcements

Bar	Yield strength (N/mm ²)	Tensile strength (N/mm ²)	Elastic modulus (kN/mm ²)	Area (mm ²)
D6	336	522	200	31.7
D10	479	498	200	71.3
D13	371	512	200	126.7

Table 2 Characteristics of concrete

Beam	Compressive strength (N/mm ²)		Tensile strength (N/mm ²)	
	Batch A	Batch B	Batch A	Batch B
SJ10-06	68.1	69.3	5.75	5.31
DSJ10-06	65.6	66.6	5.75	5.31
DSJ10-10	67.1	69.1	5.75	5.31

Note: Batch A is for large segment, Batch B is for small segment.

as shown in Fig. 2(a) and were stretched 3 days before testing. Steel deviators, located in the shear spans, were attached to the beams from the bottom to ensure that there was no change in the web thickness of the test beams. Epoxy resin was used to connect concrete segments. Prestressing was introduced after assembling concrete segments with epoxy. The compressive and tensile strengths of epoxy resin were 60 N/mm^2 and 12.5 N/mm^2 , respectively.

3.3 Loading Method and Measurements

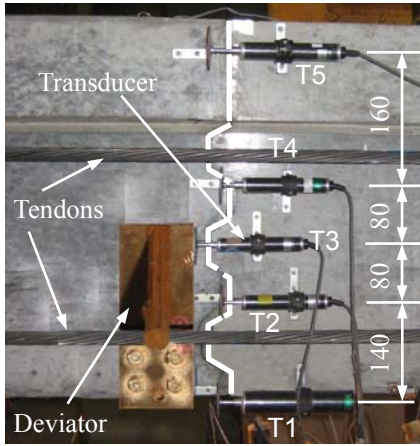
The beams were subjected to a two-point loading test with a distance of 400 mm between two loading points, as shown in Fig. 2. The applied load was increased monotonically by means of displacement control method until the beams failed.

Various measuring devices were utilized in order to measure the displacement of the beam, as well as joint opening and stress increment in the external tendons. Strain in the tendons was measured by electrical strain gauges at the middle of the external tendons. Meanwhile, displacement transducers were mounted at the midspan and the supports of the beams to monitor the vertical deflection. At the same time, transducers (T1 to T5) were placed horizontally at five levels on the segmental joints to measure the joint opening as shown in Fig. 3.

4. RESULTS AND DISCUSSION

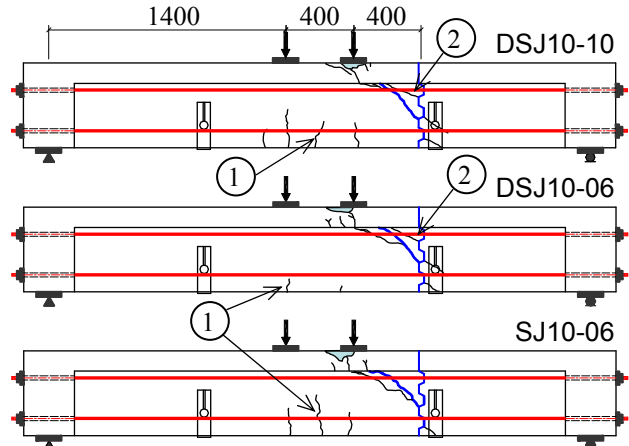
4.1 Crack Patterns and Joint Opening

Figure 4 presents the crack pattern of the beams. In DSJ10-10 and DSJ10-06, flexural cracks formed in the maximum moment zone between the loading points. The first diagonal crack formed at the lower corner of the upper key toward the loading point in the large segment. The dominant diagonal crack formed at the lower corner of the middle key in the large segment toward the loading point. At the same time as the dominant diagonal crack occurrence, cracks at the upper corner of the middle and lower keys in the small segment also formed. In SJ10-06, after the occurrence



Unit: mm

Fig. 3 Arrangement of transducers to measure joint opening



① The first flexural crack; ② The first diagonal crack
Bold line is the dominant diagonal crack

Fig. 4 Crack patterns

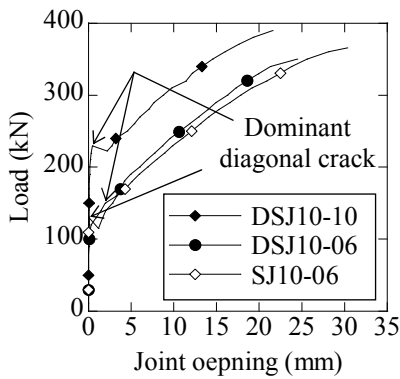


Fig. 5 Load – joint opening at lower fiber

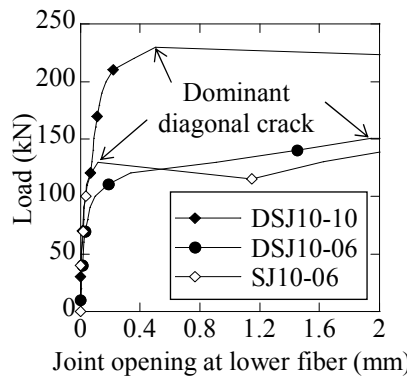


Fig. 6 Load – joint opening at lower fiber before dominant diagonal crack

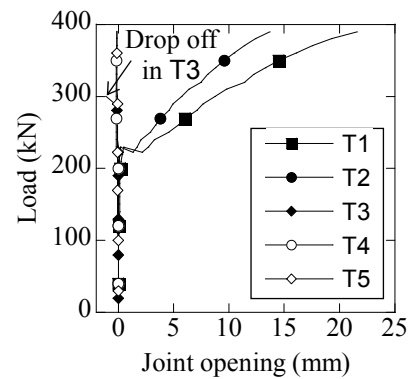


Fig. 7 Load – joint opening of DSJ10-10

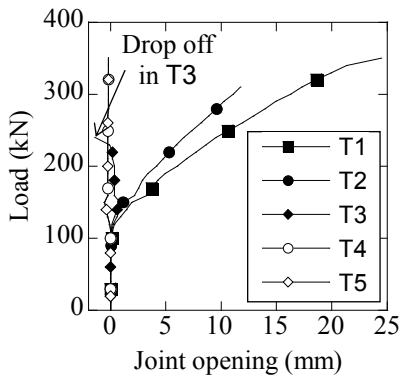


Fig. 8 Load – joint opening of DSJ10-06

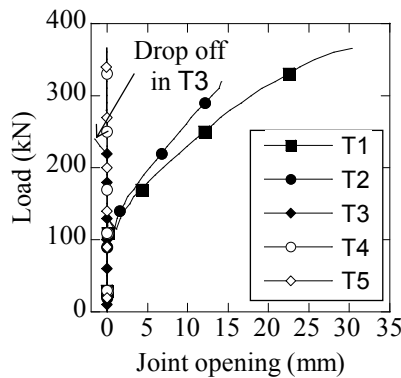


Fig. 9 Load – joint opening of SJ10-06

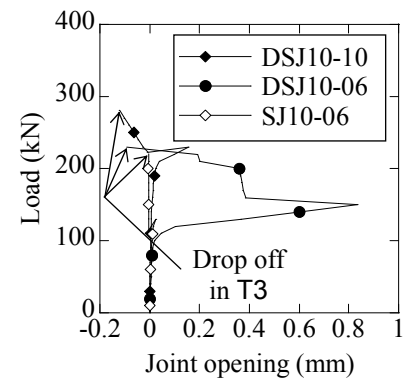


Fig. 10 Load – joint opening at level of T3

of the flexural cracks, the dominant diagonal crack formed at the lower corner of the middle key in the large segment toward the loading point.

Figure 5 presents the joint opening at the lower fiber, measured by T1 as shown in Fig. 3. In the similar prestress level, DSJ10-06 and SJ10-06, the dry joint opened more widely than the epoxy joint before the occurrence of the dominant diagonal crack as shown in Fig. 6. The joint opening at the lower fiber increased sharply as the dominant diagonal crack occurred. At the ultimate stage, the epoxy joint opened higher than the dry joint.

Figures 7, 8 and 9 show measured joint opening. The joint opening was always detected by both T1 and T2 in all tested beams. In DSJ10-10 and DSJ10-06, the joint opening was also detected by T3 until the first diagonal crack occurred as shown in Fig. 10. T3 tended to be compressed after the first diagonal crack occurred. T3 was attached fairly near to the deviator as shown in Fig. 3. So, T3 could not attain the opening value when the segments and the deviator were largely rotated. In SJ10-06, the opening value in T3 showed the joint always closed. It also dropped off as the large rotation of the segments and the deviator was observed as

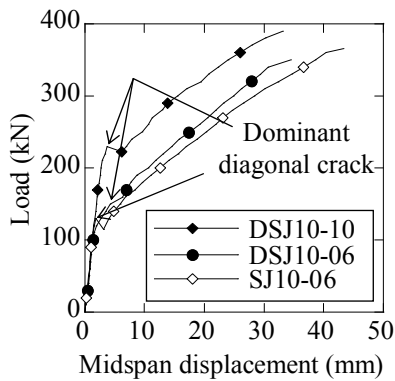
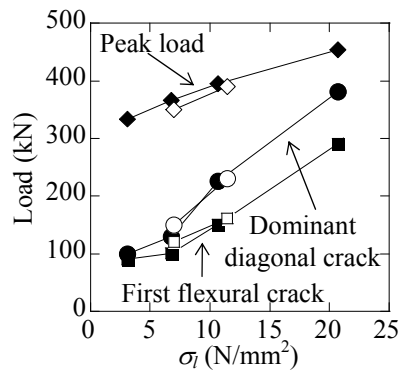


Fig. 11 Load – displacement relationship



Note: Black marks for epoxy joint, White marks for dry joint

Fig. 12 Load- σ_1 relationship



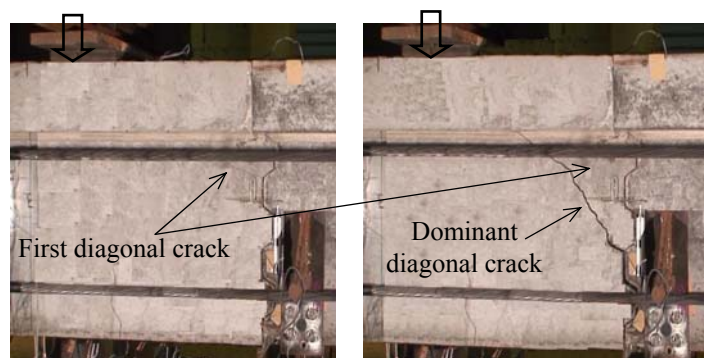
Fig. 13 Glue fiber at joint opening in SJ10-06

Table 3 Test results

Beams	P_{cr} kN	P_{sh} kN	P_u kN	JO_1 mm	JO_2 mm
SJ10-06	100	130	366.1	0.12	30.3
DSJ10-06	120	150	350.1	1.94	24.5
DSJ10-10	160	230	390.2	0.50	21.6

Note:

P_{cr} is load at first flexural crack,
 P_{sh} is load at dominant diagonal crack,
 P_u is peak load,
 JO_1 is joint opening at dominant diagonal crack,
 JO_2 is joint opening at peak load.



a) First diagonal crack

b) Dominant diagonal crack

Fig. 14 Order of diagonal cracks in DSJ10-10

shown in Figs. 9 and 10.

4.2 Load-Deflection Curves

Figure 11 illustrates load and deflection curves of tested beams. Even though there were different prestress levels and types of segmental joint, at the beginning, all segmental beams exhibited similar linear elastic behavior. Linear behavior was prolonged until the first flexural crack occurred with the loads in Table 3. The linear behavior range becomes shorter as the prestress level was reduced. A similar tendency in the effect of prestressing force was observed in the beams with dry joint and those with epoxy joint [5], as shown in Fig. 12. The loads at the first flexural crack and the dominant diagonal crack occurring in the beams with epoxy joint were smaller than those in the beams with dry joint at a similar prestress level. The ultimate capacity of DSJ10-06 was about 5% smaller than that of SJ10-06, while the ultimate capacity of DSJ10-10 was 1% smaller than that of SJ10-10 in our previous study [5].

4.3 Failure Mechanism

In SJ10-06, owing to the effect of bonding behavior of epoxy, before the occurrence of the dominant diagonal crack, joint opening was quite small, and the accumulated energy was initially dissipated by the flexural cracks. After the occurrence of these

flexural cracks, the joint opened. The joint itself opened from the lower level up to the lower corner of the middle shear key, and subsequently the dominant diagonal crack formed toward the loading point. The shear force was transferred from the large to the small segments throughout contact area of the segmental joint above the dominant diagonal crack. The failure at the base of the lower shear key [5] did not appear in SJ10-06, because the epoxy had not fully hardened yet, as shown in Fig. 13.

At similar prestress level, the load at the first flexural crack of DSJ10-06 was slightly larger than that in SJ10-06. The reason for this is that, without the bonding effect of epoxy, the joint opened broadly before the occurrence of the first flexural crack as the applied load increased, as shown in Fig. 6. Hence, the deformation of the beams with dry joint was first accumulated by the joint opening. The increase in the interlock of shear keys where the joint opened with the increase in the applied load led to the occurrence of the flexural cracks in beams with dry joint.

Then, the joint opened up to the lower corner of the upper shear key in the large segment where the first diagonal crack formed as shown in Fig. 4. The width of the first diagonal crack increased as shown in Fig. 14(a). This increased the rotation of segments, the joint opening and the interlock in the lower shear keys. At this point the dominant diagonal crack formed. The

Table 4 Evaluation of existing equations

Beam	σ_l (N/mm ²)	P_{EXP} (kN)	Modified model		AASHTO Standards		Type of joint
			P_{cal} (kN)	P_{EXP}/P_{cal}	P_{cal} (kN)	P_{EXP}/P_{cal}	
SJ10-06	6.77	366.1	333.4	1.10	240.8	1.52	Epoxy
DSJ10-06	7.01	350.1	337.5	1.04	243.1	1.44	Dry
DSJ10-10	11.46	390.2	393.9	0.99	254.6	1.53	Dry
Mean				1.04		1.50	
Standard deviation				0.044		0.041	
Coefficient of variation				0.042		0.027	

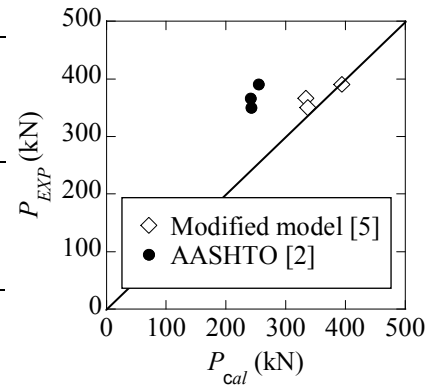


Fig. 15 Validation of equations

width of the dominant diagonal crack increased rapidly, while the width of the first diagonal crack was observed to close again as shown in Fig. 14(b). As the dominant diagonal crack occurred, the height of the opened joint above the dominant diagonal crack closed again. It increased the area to transfer the shear force from the large segment to the small segment in the beams with dry joint, as the dominant diagonal crack occurred.

Although there was a difference in the prestress level and joint types, the shear failure mode was designated in the tested beams as the shear compression failure mode. Firstly, the dominant diagonal crack was formed toward the loading point. Final failure took place with the crushing of concrete near the loading point in the shear span.

The results of this experiment shows that the shear carrying capacity of segmental concrete beams with external tendons and dry joint is approximate to that with epoxy joint. This differs from the results in direct shear test with dry and epoxy joints [3]. The shear transfer mechanism of joint in segmental beams is different from that in direct shear test. This difference is because of the effect of joint opening in segmental concrete beams.

5. EVALUATING THE EXISTING EQUATIONS

The experimental results were compared with the calculated results from the modified model [5] and the shear design provision for segmental box girder bridges included in AASHTO [2]. Table 4 and Fig. 15 show the experimental results and calculated values. It shows that the modified model is capable of predicting the shear carrying capacity of segmental beams with external tendons and dry joint. The modified model can well predict the shear carrying capacity of segmental beams with external tendon and concrete stress at the lower fiber of 6 N/mm². Comparison of the mean value shows that the shear carrying capacity obtained from the modified model displays higher accuracy than that from AASHTO for segmental beams.

6. CONCLUSIONS

- (1) The joint opening process was different between segmental concrete beams with epoxy joint and dry joint before the occurrence of the dominant

diagonal crack.

- (2) The shear failure mechanism at the ultimate stage in the segmental concrete beams with external tendons and dry joint was similar to that in the segmental concrete beams with external tendons and epoxy joint. The shear compression failure mode was observed in all the tested beams.
- (3) The modified model is capable of predicting the shear carrying capacity of segmental beams with external tendons and dry joint. The modified model can also predict the shear carrying capacity of segmental beams with external tendon and concrete stress at the lower fiber of 6 N/mm².

REFERENCES

- [1] C. Burgoyne and R. Scantlebury: Lessons Learned from the Bridge Collapse in Palau, Proceedings of the ICE, Civil Engineering, Vol. 161, No. 6, pp. 28-34, 2008.
- [2] AASHTO: Guide Specifications for the Design and Construction of Segmental Concrete Bridges, 2nd Edition, Washington, D.C., pp. 3-118, 1999.
- [3] X. Zhou, N. Mickleborough and Z. Li: Shear Behavior of Joints in Precast Concrete Segmental Beams, ACI Structure Journal, Vol. 102, No. 11, pp. 3-11, 2005.
- [4] Z. Kamaitis: Field Investigation of Joints in Precast Post-Tensioned Segmental Concrete Bridges, Baltic Journal of Road and Bridge Engineering, Vol. 3, No. 4, pp. 198-205, 2008
- [5] D. H. Nguyen, K. Watanabe, J. Niwa and T. Hasegawa: Modified Model for Shear Carrying Capacity of Segmental Concrete Beams with External Tendons, Journal of Materials, Concrete Structures and Pavements, JSCE, Vol. 66, No. 1, pp. 53-67, 2010.
- [6] M. Lertsamattiyakul: Simplified Truss Model for Shear Carrying Capacity of Prestressed Concrete Members, PhD Thesis, Tokyo Institute of Technology, 2005.
- [7] C. Sevalepunth, J. Niwa, D. H. Nguyen, T. Hasegawa and Y. Hamada: Shear Carrying Capacity of Segmental Prestressed Concrete Beams, Journal of Materials, Concrete Structures and Pavements, JSCE, Vol. 65, No. 1, pp. 63-75, 2009.